Biochem. J. (2015) **471**, 211–220 doi:10.1042/BJ20150730

Methylation of the *Gpat2* promoter regulates transient expression during mouse spermatogenesis

Maria B. Garcia-Fabiani*, Mauro A. Montanaro*, Ezequiel Lacunza†, Elizabeth R. Cattaneo*, Rosalind A. Coleman‡, Magali Pellon-Maison* and Maria R. Gonzalez-Baro*[1]

*Instituto de Investigaciones Bioquímicas de La Plata, Consejo Nacional de Investigaciones Científicas y Técnicas, Facultad de Ciencias Médicas, Universidad Nacional de La Plata, La Plata 1900, Argentina

†Centro de Investigaciones Inmunológicas Básicas y Aplicadas, Facultad de Ciencias Médicas, Universidad Nacional de La Plata, La Plata 1900, Argentina

‡Department of Nutrition, University of North Carolina, Chapel Hill, NC 27599, U.S.A.

Spermatogenesis is a highly regulated process that involves both mitotic and meiotic divisions, as well as cellular differentiation to yield mature spermatozoa from undifferentiated germinal stem cells. Although *Gpat2* was originally annotated as encoding a glycerol-3-phosphate acyltransferase by sequence homology to *Gpat1*, GPAT2 is highly expressed in testis but not in lipogenic tissues and is not up-regulated during adipocyte differentiation. New data show that GPAT2 is required for the synthesis of piRNAs (piwi-interacting RNAs), a group of small RNAs that protect the germ cell genome from retrotransposable elements. In order to understand the relationship between GPAT2 and its role in the testis, we focused on *Gpat2* expression during the first wave of mouse spermatogenesis. *Gpat2* expression was analysed by qPCR (quantitative real-time PCR), *in situ* hybridization, immunohistochemistry and Western blotting. *Gpat2* mRNA content and protein expression were maximal at 15 dpp (days post-partum) and were restricted to pachytene spermatocytes. To achieve this transient expression, both epigenetic mechanisms and *trans*-acting factors are involved. *In vitro* assays showed that *Gpat2* expression correlates with DNA demethylation and histone acetylation and that it is up-regulated by retinoic acid. Epigenetic regulation by DNA methylation was confirmed *in vivo* in germ cells by bisulfite sequencing of the *Gpat2* promoter. Consistent with the initiation of meiosis at 11 dpp, methylation decreased dramatically. Thus, *Gpat2* is expressed at a specific stage of spermatogenesis, consistent with piRNA synthesis and meiosis I prophase, and its on–off expression pattern responds predominantly to epigenetic modifications.

Key words: epigenetic regulation, GPAT2, meiosis, retinoic acid.

INTRODUCTION

Spermatogenesis is a highly regulated process that involves both mitotic and meiotic divisions, as well as cellular differentiation to yield mature spermatozoa from undifferentiated germinal stem cells. The endocrine regulation of spermatogenesis occurs through the combined action of hormones and growth factors, including the effects of retinoic acids (RAs), which are vitamin A derivatives essential for meiosis initiation [1,2]. Epigenetic modifications and chromatin remodelling are also important regulators in spermatogenesis [3]. PIWI-interacting RNAs (piRNAs) are small non-coding RNAs synthesized in germ cells, where they are believed to repress the expression of deleterious retrotransposons, thereby ensuring genome integrity during meiosis [4]. In mice these small non-coding RNAs interact with the Argonaute family proteins (Ago and PIWI clades of proteins), such as MIWI, MILI and MIWI2 members, which also participate in piRNA biogenesis. Glycerol-3-phosphate acyltransferase-2 (GPAT2) was unexpectedly found to be required for piRNA biogenesis. The knockdown of *Gpat2* in germline stem cells impairs primary piRNA production, and it was shown that the GPAT2 protein physically interacts with MILI in both germline stem cells and mouse testis. The mechanism by which GPAT2 promotes piRNA production remains unknown, but because this function occurs despite the absence of the acyltransferase motif, $H(X_4)D$, the regulation of piRNA production by GPAT2 is unlikely to require acyltransferase enzymatic activity [5].

GPAT isoforms catalyse the first and rate-limiting step in *de novo* glycerolipid biosynthesis, acylating glycerol 3-phosphate with a long-chain fatty acyl-CoA to form lysophosphatidic acid (LPA). LPA is the substrate for 1-acylglycerol-3-phosphate acyltransferase which catalyses the formation of phosphatidic acid, the precursor for triacylglycerol and glycerophospholipid biosynthesis. In mammals, four GPAT isoforms (GPAT1–GPAT4) have been described which differ in their subcellular locations, tissue expression pattern, substrate preference, transcriptional regulation and sensitivity to sulfhydryl group reagents such as *N*-ethylmaleimide [6]. GPAT1 and GPAT2 are mitochondrial isoforms, whereas GPAT3 and GPAT4 are located in the endoplasmic reticulum. GPAT1, GPAT3 and GPAT4 are highly expressed in lipogenic tissues such as liver and adipose tissue where they initiate the *de novo* synthesis of triacylglycerol and glycerophospholipids [6]. During adipocyte differentiation of 3T3-L1 fibroblasts, the expression of these three isoforms increases; *Gpat1* and *Gpat4* are moderately induced (10- and 5-fold, respectively) in differentiated adipocytes and *Gpat3* is highly induced (>60-fold) [7–9]. In contrast, *Gpat2* mRNA expression is not regulated by nutritional status, and it is at least 50-fold higher in testis than in any other tissue [10].

Abbreviations: ATRA, all-*trans*-RA; CHO, Chinese-hamster ovary; 9cisRA, 9-*cis*-retinoic acid; CTs, cancer-testis genes; DAC, 5-aza-2-deoxycitidine; DMEM, Dulbecco's modified Eagle's medium; dpc, days post-coitum; dpp, days post-partum; fRMA, frozen robust multi-array analysis; GPAT, glycerol-3-phosphate acyltransferase; IHC, immunohistochemistry; LPA, lysophosphatidic acid; piRNA, PIWI-interacting RNA; qPCR, quantitative real-time PCR; RA, retinoic acid; RAR, RA receptor; TSA, trichostatin A; VDAC, voltage-dependent anion channel.

[1] To whom correspondence should be addressed (email mgbaro@med.unlp.edu.ar).

GPAT2 also differs from the other GPAT isoforms in that it belongs to a group of genes named 'cancer-testis genes' (CTs). CTs are important at specific stages during spermatogenesis, but are expressed at low levels or not expressed at all in somatic tissues. CTs are ectopically overexpressed in cancers from different locations, and contribute to the tumour phenotype [11,12]. We have shown that human GPAT2 is overexpressed in several types of cancer and in cancer-derived human cell lines, and that its expression contributes to the tumour phenotype, because in tumour cells with diminished GPAT2 expression, the proliferation and migration rates are lower, and in mouse xenograft models, cells with diminished GPAT2 expression have lower tumorigenicity [13].

To understand the physiological role of GPAT2 in the testis, we focused on its developmental regulation during spermatogenesis. Our data show that *Gpat2* is expressed at a specific stage of the spermatogenesis, consistent with meiosis I prophase and that its on–off expression pattern responds predominantly to epigenetic modifications and probably to RA signalling.

MATERIALS AND METHODS

Chemicals

All chemicals were purchased from Sigma unless otherwise indicated.

Animals, cell lines and culture conditions

Animal protocols were approved by the Facultad de Ciencias Médicas, Universidad Nacional de La Plata Institutional Animal Care and Use Committee (Approval Number T10-02-2013). Male BALB/c mice were housed on a 12-h light/12-h dark cycle with free access to water and Cargill Rodent chow. Before testis dissections, mice were killed in a CO_2 chamber. Cells were purchased from A.T.C.C. and were grown at 37 °C in a 5 % CO_2 atmosphere with a 98 % relative humidity. The hamster cell line CHO (Chinese-hamster ovary)-K1 was maintained in Ham's F12 (Gibco) medium, the mouse macrophage cell line RAW 264.7 and the embryonic fibroblast 3T3-L1 mouse cell line in Dulbecco's modified Eagle's medium (DMEM) (Gibco), the human breast cancer cell line derived from metastatic pleural effusion MCF7 in RPMI 1640 medium (Gibco) and the mouse Sertoli cell line TM4 in DMEM/Ham's F12 (Gibco). All media were supplemented with 10 % FBS and antibiotics (50 units/ml penicillin and 50 μg/ml streptomycin).

Analysis of mRNA transcription

Total RNA from BALB/c mouse testes at 3, 7, 11, 15, 20, 35 and 50 days post-partum (dpp), RAW 264.7 and 3T3L1 cells was isolated with TRIzol Reagent (Invitrogen) according to the manufacturer's instructions. RNA quality was determined by gel electrophoresis and 260/230 and 260/280 nm absorbance ratios. A 1 μg sample of total RNA was used for cDNA synthesis employing the High Capacity Reverse Transcription Kit (Applied Biosystems). A 1/15 cDNA dilution was used for the qPCR (quantitative real-time PCR) with ABsolute QPCR SYBR Green Mix (Thermo). Primers were designed to amplify a fragment of 187 bp between exon 16 (forward primer: 5′-ATCCTACTGCTGCTGCACCT-3′) and exon 18 (reverse primer: 5′-ACAGCAGCTTTGCACTCAGA-3′) of the mouse *Gpat2* transcript. The thermal profile was 95 °C for 15 min, followed by 40 cycles of 95 °C for 30 s, 55 °C for 1 min and 72 °C for 30 s, on a Stratagene Mx3000P apparatus. RNA expression was quantified in duplicate using the $\Delta\Delta C_T$ method, and each sample was normalized to two different housekeeping genes: *Gapdh* (forward primer: 5′-CTGGAGAAACCTGCCAAGTA-3′; reverse primer: 5′-TGTTGCTGTAGCCCGTATTCA-3′) and *Rpl13a* (forward primer: 5′-ATGACAAGAAAAAGCGGATG-3′; reverse primer: 5′-CTTTTCTGCCTGTTTCCGTA-3′) using qBase software.

In silico evaluation of mouse *Gpat2* expression

To validate experimental results regarding the *Gpat2* mouse expression profile during testis development, microarray data from pre- and post-natal ages were collected to construct a box plot graphic. Gene expression information was obtained from GSE4818 ($n = 21$, mouse testis prenatal development) and GSE12769 ($n = 20$, mouse testis postnatal development) datasets, both developed in the Affymetrix genechip mouse genome 430 2.0 platform (Mouse430_2). To generate a homogeneous dataset in fetal and adult mouse testes, the frozen robust multi-array analysis (fRMA) package from Bioconductor (http://www.bioconductor.org/) was employed. The fRMA preprocessing algorithm allows the analysis of independent oligo-microarray studies/batches, and then combines the data for further statistical analysis. *Gpat2* mRNA expression level was estimated by using the expression values of the Affymetrix probe 1456208_AT.

In situ hybridization

Riboprobes for *in situ* hybridization were prepared by digesting mouse *Gpat2* cDNA from the pcDNA3.1-Gpat2 construct at the BamHI and EcoRI sites and subcloning the 1456 bp fragment into pGEM11z(f)+ vector (Promega). The tissue preparation, probe synthesis and hybridization were performed at the University of North Carolina at Chapel Hill Neuroscience Center Molecular Neuroscience Core Facility (http://www.med.unc.edu/neuroscience/core-facilities/molecular-neuroscience). Testes from 7, 15 and 30 dpp mice were fixed in 4 % paraformaldehyde in 0.1 M PBS, and processed as previously described [14]. Slides were visualized in an Olympus BX52 microscope.

Immunohistochemistry analysis

Testes from 7, 15, 30 and 40 dpp mice were fixed in Bouin's solution in the same paraffin block, and 4 μm sections were cut. Samples were processed as previously described [14]. Slides were counter-stained with haematoxylin to visualize the nuclei and analysed with an Olympus BX52 microscope.

3T3-L1 differentiation assay

3T3-L1 cells were seeded in 12-well plates and grown in routine medium until confluence, then stimulated with 2 μg/ml insulin, 0.25 μM dexamethasone and 0.5 mM isobutylmethylxanthine (IBMX) [15]. Full differentiation was achieved on day 8. RNA (triplicate samples) was isolated with TRIzol Reagent at different times: 0, 12, 18, 24, 36, 48, 96, 144 and 192 h. A 1 μg sample was used for cDNA synthesis, and *Gpat2* content was evaluated by qPCR.

Cloning of *Gpat2* gene promoter regions

Primer pairs were used to amplify different regions of the putative *Gpat2* promoter upstream of the ATG start codon from mouse genomic DNA; all included a terminal MluI (forward primer) or HindIII (reverse primer) restriction sites. Forward primers: −1324P fragment (−1324/+2105) 5′-ACGCGTGGTTCTG-AAACTGGAGGTCAG-3′, −1165P fragment (−1165/+2105)

5′-ACGCGTGACCAGGAGAGGGTGCTAGA-3', −873P fragment (−873/+2105) 5′-ACGCGTACAGCTGACCAAAAGCCACT-3′, −642P fragment (−642/+2105) 5′-ACGCGTTGGGGTAATTGGTTCTCACC-3′, −156P fragment (−156/+2105) 5′-ACGCGTTGTGGTACAGGCAGCAAGTC-3′ and +165P fragment (+165/+2015) 5′-ACAGTCAGAGGCAAGCTGGT-3′. The reverse primer was 5′-AAGCTTTCTGTAAGATCAGTGAATCAAGCAC-3′. To test for possible downstream regulation, the first non-translated exon of *Gpat2* mRNA as well as the first intron were included in the promoter constructs [16]. All five fragments were amplified using iProof High-Fidelity DNA Polymerase (Bio-Rad Laboratories), double digested with MluI and HindIII and ligated into the pGL3-Basic Vector (Promega). All plasmids were prepared using the Plasmid Miniprep kit (Qiagen), quantified by UV spectrophotometry and sequenced.

Cell transfection, hormone response evaluation and luciferase assay

To study basal promoter activity, CHO-K1 cells were seeded in a 24-well plate. The next day Lipofectamine 2000 (Invitrogen) was used to co-transfect 0.5 μg/well of each pGL3 construct with 0.05 μg/well of pRL-*Renilla* Luciferase Reporter Vector (*Renilla*). Thirty-six hours after transfection, cells were harvested and lysed and luciferase activity was measured using the Dual-Luciferase Reporter Assay System (Promega). Relative luciferase activity was normalized by the *Renilla* luciferase activity. To evaluate the hormone response, CHO-K1, MCF7 or TM4 cells were seeded in a 48-well plate 24 h before Lipofectamine 2000 co-transfection with 1.14 μg/well of pGL3 constructs and 0.11 μg/well of *Renilla* luciferase plasmid. Five hours after transfection, medium with hormones and lacking FBS, was added to the cells. The next day, the medium was replaced with fresh medium and hormones. Forty-eight hours after transfection, cells were harvested and lysed and luciferase activity was measured as described above. All experiments were performed in duplicate and repeated at least twice. Hormones tested (concentration range is indicated within parentheses): oestradiol (0.1–10 nM), corticosterone (0.1–0.2 μM), all-*trans*-retinoic acid (ATRA) (2–20 μM) and 9-*cis*-retinoic acid (9cisRA) (2–8 μM).

DAC and TSA treatments

The effect of the DNA methyltransferase inhibitor 5-aza-2-deoxycitidine (DAC) and the histone deacetylase inhibitor trichostatin A (TSA) on *Gpat2* transcription was studied in RAW 264.7 cells. Cells were seeded in a 12-well plate to reach 20 % confluence. The next day, the medium was changed, and cells were treated with 2 μM DAC (for 'DAC' and 'TSA + DAC' treatments) or DMSO (control). Media and DAC were replaced every 24 h for 3 days. TSA (500 nM) was added on the fourth day ('TSA' and 'TSA + DAC' treatments) and cells were harvested on day 5. Total RNA was isolated using TRIzol Reagent (Invitrogen); 1 μg was used for cDNA synthesis and *Gpat2* mRNA content was measured by qPCR. Each treatment was performed twice in triplicate.

In vitro methylation

The −156P *Gpat2* promoter construct (3 μg/reaction) was incubated with 160 μM *S*-adenosylmethionine (SAM) and 10 units of SssI methylase (CpG methyltransferase, M.SssI, New England Biolabs) ('methylated') or without enzyme ('unmethylated') for 4 h at 37 °C, followed by a 20 min inactivation at 60 °C. Plasmids were purified using the commercial kit Illustra GFX PCR DNA and Gel Band Purification Kit (GE Healthcare Life Sciences) and Lipofectamine 2000 (Invitrogen) was used to co-transfect with *Renilla* luciferase plasmid into CHO-K1 cells. The next day, cells were harvested and luminescence was measured using the Dual-Luciferase Reporter Assay System (Promega) and normalized to that of *Renilla*.

Germ cell purification

Germ cells were isolated from testes of mice at 11, 15 and 30 dpp as described in [17]. Cells were incubated overnight at 34 °C in 4 % CO_2 to allow Sertoli cells to adhere to the culture plate surface. The germ-cell-enriched supernatant was removed, and centrifuged for 10 min at 800 ***g*** at room temperature, and then genomic DNA was extracted from the pellet.

Bisulfite treatment and sequencing

Using DNeasy Blood & Tissue Kit (Qiagen), total DNA was purified from whole testis from 7 dpp mice and from germ cells isolated from mouse testis at selected ages. DNA purity and concentration were evaluated using a NanoDrop spectrophotometer (Thermo Scientific). For bisulfite treatment, 2 μg of genomic DNA was treated employing the EpiTect Bisulfite Kit (Qiagen). PCR was performed using Taq DNA polymerase (Invitrogen); the protocol was similar to a nested PCR, but using the same set of primers. For each reaction, 100 ng of bisulfite-converted DNA was used, and cycling conditions were: 2 min at 94 °C for initial denaturation, followed by a touchdown step of eight cycles of 45 s at 94 °C, 40 s at 64–56 °C, 1.5 min at 72 °C; 30 cycles of 45 s at 94 °C, 40 s at 56 °C, 1.5 min at 72 °C and a final extension step of 6 min at 72 °C. Samples of 5 μl of these PCR products were then used as templates with the same reaction conditions. Primers used were: forward: 5′-ATTGGTTGGTTTTTTAGTTGTTGAG-3′; reverse: 5′-ATTCCACATCAATCCCTACCTAAC-3′. The products of interest (197 bp) were gel purified with the Illustra GFX PCR DNA and Gel Band Purification Kit, ligated into pGEMT-Easy Vector (Promega) and transformed into *Escherichia coli* JM109 competent cells. Insertion was confirmed by restriction enzyme digestion, and eight clones were chosen for sequencing.

Mouse testis subcellular fractionation and immunoblotting

Testes from 7, 15, 20 and 35 dpp BALB/c mice were removed, rinsed with ice-cold PBS and submerged in precooled buffer H [10 mM Hepes/KOH, pH 7.4, 0.25 M sucrose, 1 mM EDTA, 1 mM DTT, 0.002 % protease inhibitor cocktail (general use) 1:6 (w/v)]. Testes were homogenized with ten up-and-down strokes in a motor-driven Teflon-glass vessel. Large debris and nuclei were pelleted by centrifuging twice at 600 ***g*** for 5 min. The supernatant (post-nuclear homogenate) was centrifuged for 10 min at 10000 ***g***. The pellet was resuspended in 1 ml of buffer H/g of testis and homogenized in a Dounce tissue grinder with a glass pestle to obtain a mitochondria-enriched protein fraction.

Samples of 100 μg of the mitochondria-enriched protein fractions were separated by SDS/PAGE (8 or 12 % gel), transferred to a PVDF membrane (Bio-Rad Laboratories) and probed with a 1:500 dilution of anti-GPAT2 antibody [14] or with 1:2000 of the anti-voltage-dependent anion channel (VDAC) antibody (Affinity Bioreagents), as loading control. Membranes were then washed extensively and probed with 1:5000 dilution of horseradish peroxidase-conjugated goat anti-rabbit

IgG antibody (Thermo-Pierce). For chemiluminescent detection, the membranes were incubated with Super Signal detection kit (Thermo-Pierce).

RESULTS AND DISCUSSION

Gpat2 mRNA and protein are highly expressed in pachytene spermatocytes

GPAT2 is expressed in male germ cells, particularly in primary spermatocytes, and its expression changes during rat sexual development [14]. The first round of spermatogenesis in mammals is characterized by the synchronized appearance of particular cell types at different stages of the spermatogenic cycle among the seminiferous tubules, and this model was used to analyse differential gene expression during spermatogenesis [18,19]. In mouse testis, only Sertoli cells and spermatogonia populate the seminiferous tubules until 10 dpp. Subsequently, meiotic cells appear in the tubules: at 11 dpp meiosis advances no further than the zygotene stage, at 13 dpp to the early pachytene, at 15 dpp to the middle pachytene, at 18 dpp to the late pachytene, at 20 dpp to the round spermatid stage and at 30 dpp spermatids have already reached the elongation phase and sperm tail accessory structures are being constructed. After this period, synchrony is lost and all stages of spermatogenesis can be observed; however, apart from mature spermatozoa, pachytene spermatocytes and round spermatids remain the most abundant germ cell types in seminiferous tubules [20]. In order to study the relative expression of *Gpat2* mRNA during the first wave of spermatogenesis, total RNA was extracted from testis at selected ages and expression was assessed by qPCR (Figure 1A). The mRNA content was low at 3 and 7 dpp, and then increased, reaching a peak at 15 dpp, after which expression fell by 50 % to a value that remained unchanged throughout adulthood. To evaluate mRNA expression in the seminiferous tubules, *in situ* mRNA hybridization was performed on slides of mouse testis at 7, 15 and 30 dpp (Figure 1C). The label was undetectable at 7 dpp, but positive staining was observed at 15 and 30 dpp. Strong labelling was observed at 15 dpp and most cells populating the tubules were positive for *Gpat2* mRNA, except for the basal germ cells corresponding to spermatogonia. In contrast, at 30 dpp the label was detected only in primary spermatocytes, and mRNA expression was abruptly extinguished in the subsequent stages of spermatogenesis. These results are consistent with the analysis of microarray data collected from mouse testis, from fetal age to adulthood (duplicates in 11, 12, 14, 16 and 18 days post-coitum (dpc), 0, 3, 6, 8, 10, 14, 18, 20, 30 and 35 dpp) which shows the time course of gene expression in murine testis development (GEO Datasets: GDS2098 and GSE12769). Postnatal *Gpat2* followed a similar profile to the one described in the present study (Figure 1B), and the microarray data demonstrated that *Gpat2* transcription is transiently active during embryonic development, reaching a peak at 15 dpc (Figure 1B).

To verify GPAT2 protein expression, Western blot analysis and immunohistochemistry (IHC) were performed. Western blotting showed that the protein expression peaked at day 20, consistent with the high transcriptional rate at 15 dpp and the moderate transcription level at 20 dpp (Figure 2A). IHC was also performed on mouse testes at 7, 15, 30 and 40 dpp (Figure 2B). Similar to the mRNA expression pattern, GPAT2 protein was undetectable in 7 dpp testis, whereas a positive cytoplasmic signal was detected in testes from 15, 30 and 40 dpp mice. Again, the distribution of the signal varied among the different germ cells within the seminiferous tubules. Strong staining was present in nearly all spermatocytes at 15 dpp (when pachytene spermatocytes predominate). This stain was localized to pachytene spermatocytes at 30 and 40 dpp and became more diffuse in later stages of spermatogenesis (Figure 2B). Thus, *Gpat2* mRNA expression and maximum GPAT2 protein content within adult testis were restricted to pachytene spermatocytes. This temporospatial profile suggests that GPAT2 plays a specific role in spermatogenesis and that strict transcriptional regulatory mechanisms operate to ensure an on–off expression pattern. The specific role for GPAT2 in spermatogenesis is suggested by its involvement in the metabolism of a class of small non-coding RNAs called piRNAs that are predominantly synthesized in germ cells; *Gpat2* silencing in germline stem cells severely impaired primary piRNA production. In addition, in both germline stem cells and testis, GPAT2 interacts with MILI protein, a key player in piRNA metabolism [5]. The expression of piRNAs in mouse testis occurs at two distinct phases: pre-pachytene piRNAs are present in fetal mice, are enriched in transposon sequences, and are synthesized by the primary and secondary (‘ping-pong’) pathways, whereas pachytene piRNAs originate from discrete genomic loci (piRNA clusters), and their synthesis is independent of the ping-pong cycle [21,22]. This expression profile of *Gpat2* reinforces the idea that GPAT2 functions in the primary piRNA biosynthesis pathway, since *Gpat2* expression peaks not only when both pre-pachytene (embryonic) and pachytene piRNA are synthesized, but also occurs simultaneously with *Mili* transcription (GEO Datasets: GDS2098 and GSE12769).

Evaluation of *Gpat2* minimal promoter

Epigenetic modifications operate with *trans*-acting factors to achieve transient gene expression and ensure the progression of spermatogenesis. To identify the promoter region and study the regulatory elements of the *Gpat2* gene, the 5′ sequence flanking the transcription start site (TSS) (−1320 to translation start site) was analysed by online programs and applications, such as GPMiner, Alibaba 2.0, MethPrimer and Epigenomics (NCBI) to recognize promoter elements such as the TATA box, CCAAT box and GpC islands. The first intron was included because in other genes, transcription factor-binding sites or CpG islands are present in this region [16,23]. The *Gpat2* promoter lacked a canonical TATA box and/or CAAT boxes in the 5′-flanking region, but a CpG island containing ten CpG pairs was detected from -92 to $+32$. These features are characteristic of a ‘CpG island promoter’ class [24]. To establish the region of minimal promoter activity, serial deletions of the putative promoter region were made, cloned into a luciferase reporter vector and transiently transfected into CHO-K1 cells. Basal transcription promoter activity was located between −156 and +1 position (Figure 3), a sequence that contains three potential binding sites for Sp1 (specificity protein 1, which can initiate transcription when the TATA box is absent [24]) and the CpG island described above. These constructs were used to evaluate the influence of CpG methylation or hormones on *Gpat2* promoter activity.

Methylation status of *Gpat2* promoter changes during the first wave of spermatogenesis

qPCR and *in situ* hybridization experiments during the first wave of spermatogenesis demonstrated that *Gpat2* mRNA transcription occurred transiently in meiotic cells; expression was higher in pachytene spermatocytes and abruptly decreased in subsequent stages of spermatogenesis. We previously speculated that ectopic GPAT2 expression in human cancer cells could be the consequence of epigenetic modifications [13]. Thus, because

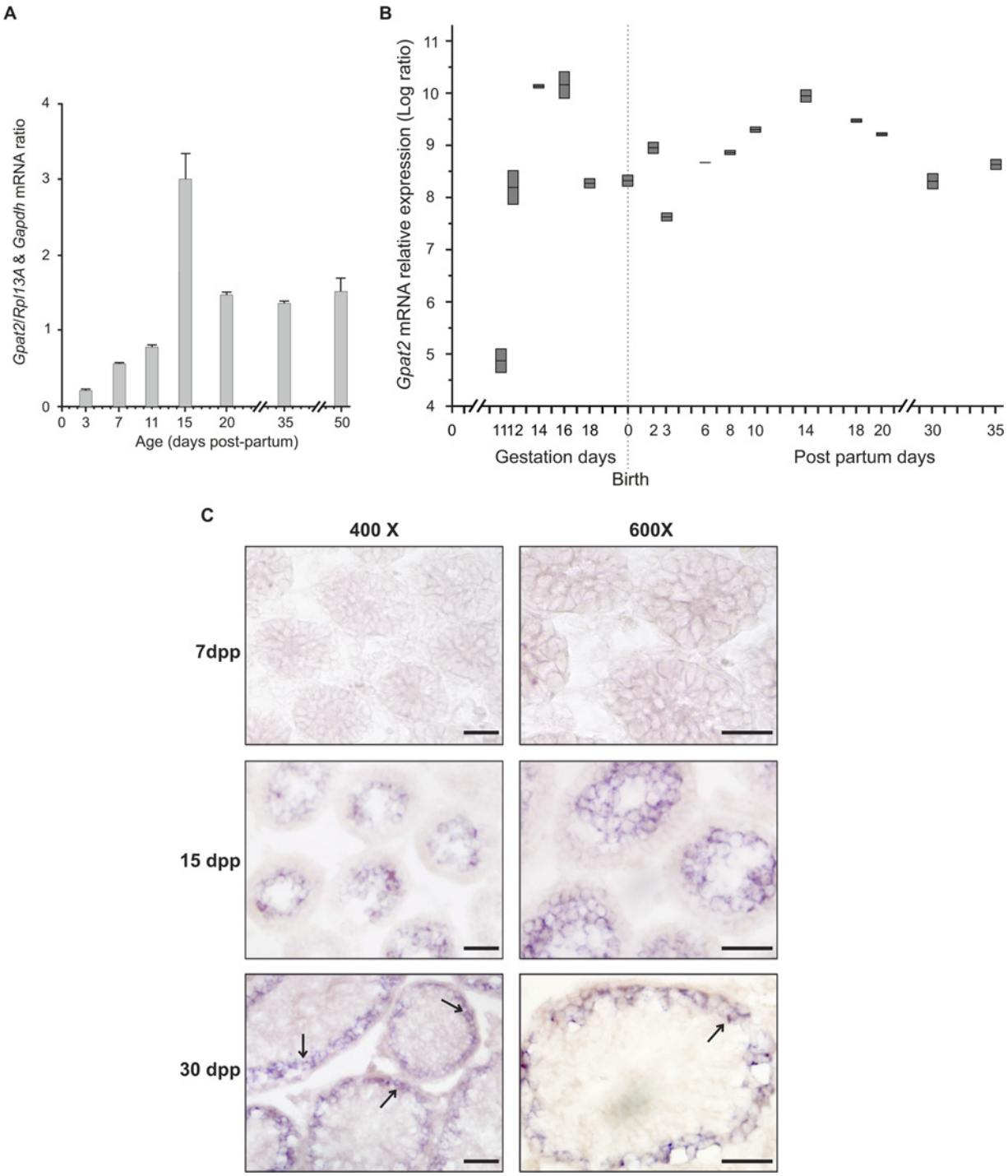

Figure 1 ***Gpat2*** **mRNA expression analysis during the first wave of spermatogenesis**

(**A**) *Gpat2* mRNA content was analysed in mouse testis at selected ages and the *Gpat2* mRNA relative expression level for each sample was normalized to both *Gapdh* and *Rpl13A* mRNA expression level. (**B**) *In silico* analysis of pre- and post-natal *Gpat2* expression was performed using microarray information obtained from the public database GEO Profiles (NCBI). (**C**) mRNA expression was assayed by *in situ* hybridization performed on slides of 7, 15 and 30 dpp mouse testis. Arrows indicate positive reaction. Scale bar = 50 μm.

epigenetic events are critical in regulating spermatogenesis, we asked whether these mechanisms could regulate *Gpat2* transcription during mouse spermatogenesis. To answer this question, we first assayed the effect of chromatin modification reagents such as the DNA methyltransferase inhibitor DAC and the histone deacetylase inhibitor TSA on *Gpat2* transcription. The murine cell line RAW 264.7 expresses low basal levels of *Gpat2*, but DAC treatment induced *Gpat2* expression 2-fold ($P < 0.01$), whereas TSA treatment did not change mRNA expression. The combination of both TSA and DAC treatments enhanced *Gpat2* transcription almost 6-fold (Figure 4A), illustrating synergistic effects on *Gpat2* transcription. These experiments demonstrate

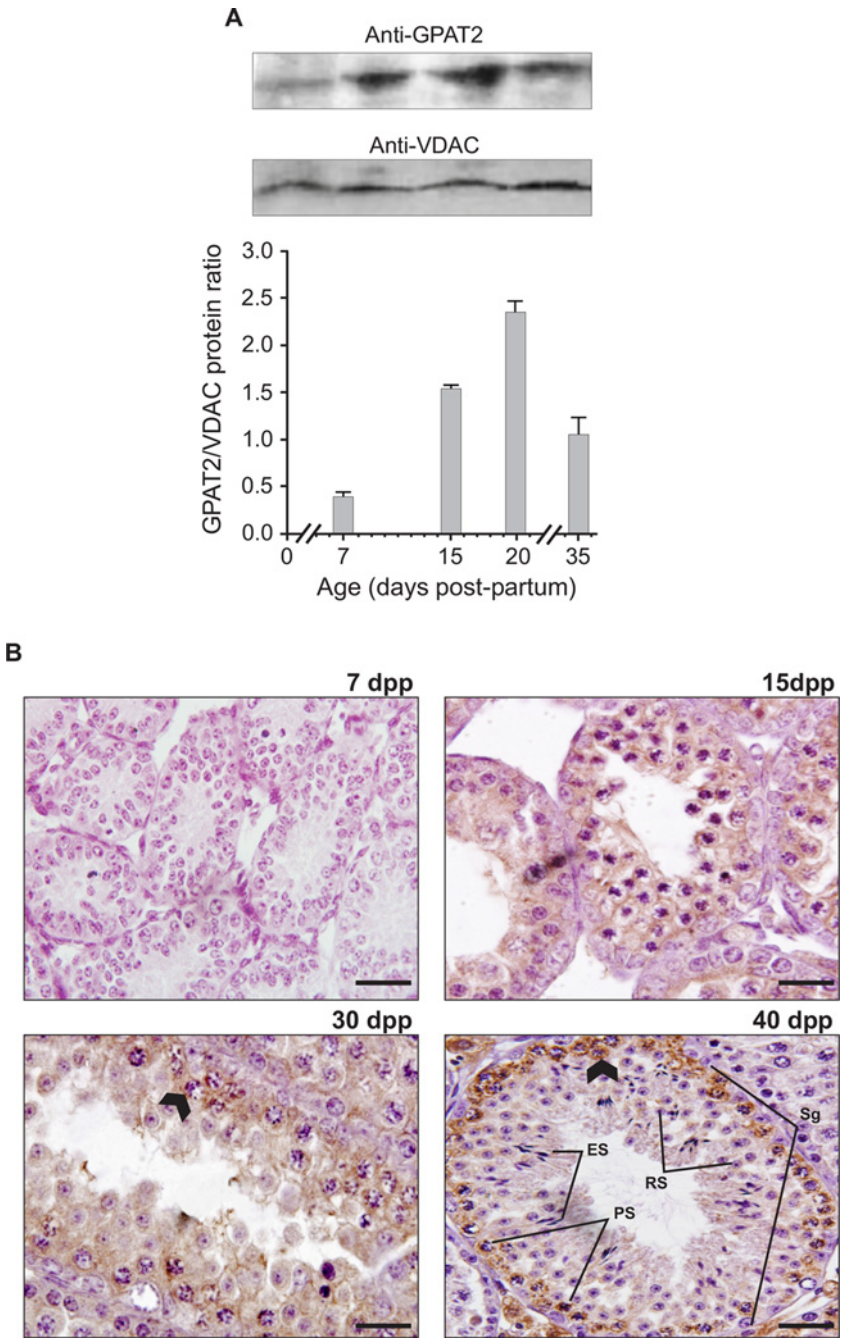

Figure 2 GPAT2 protein expression analysis during the first wave of spermatogenesis

(**A**) GPAT2 protein content was analysed in testis mitochondrial fractions extracted at selected ages and normalized to the expression of the mitochondrial VDAC. Results are expressed as the means for three independent experiments ± S.D. (**B**) IHC was assessed in 7, 15, 30 and 40 dpp mouse testis (×600 magnification). Arrowheads indicate the germ cells showing a strong signal at 30 and 40 dpp. Scale bar = 50 μm. Sg, spermatogonia; PS, pachytene spermatocytes; RS, round spermatids; ES, elongating spermatids. Scale bar = 50 μm.

that epigenetic changes such as hypomethylation, have a profound effect on the rate of *Gpat2* transcription and that the modifications on histone acetylation become important when methylation is low. This result is consistent with microarray data showing that mice null for histone deacetylase 2 highly up-regulate *Gpat2* expression in the heart, a tissue in which *Gpat2* is not constitutively expressed (GEO profile GDS2624/1456208_at/*Gpat2*). To determine whether methylation has the opposite effect on the *Gpat2* promoter, i.e. methylation is associated with *Gpat2* silencing, the construct −156P containing the minimal promoter of *Gpat2* and the typical CpG island located between −92 and +32, was methylated *in vitro* and luciferase activity was assayed (Figure 4B). Unmethylated construct activity was 20-fold higher than the internal *Renilla* luciferase control, whereas methylated construct activity was lower than the internal control (10% of the activity), suggesting that CpG methylation of the *Gpat2* minimal promoter prevents transcription. In summary, whereas DNA hypomethylation and histone acetylation are associated with

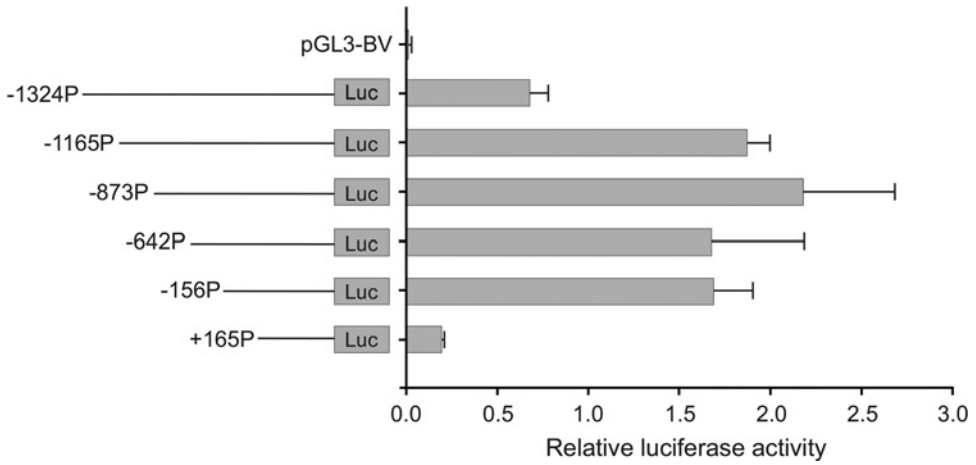

Figure 3 Basal promoter activity of the murine *Gpat2* gene

Serial deletions of the putative promoter region were made, cloned into luciferase vector and transiently transfected into CHO-K1 cells. Relative luciferase activity was normalized to the *Renilla* luciferase internal control. Results are expressed as the means ± S.D. of replicates from two independent experiments.

high transcription rates, DNA methylation of the *Gpat2* promoter prevents transcription.

To elucidate the methylation status of the *Gpat2* promoter *in vivo*, total genomic DNA was purified from 7 dpp mouse testis and from germ cells isolated from mice at 11, 15 and 30 dpp. At 7 dpp all clones were fully methylated, at 11 dpp a dramatic hypomethylation occurred in all the CpG pairs within the island, and at 15 dpp all clones were remethylated (Figure 4C). Interestingly, at 30 dpp (when primary and secondary spermatocytes populate the tubules) the clones presented an on–off pattern: the CpG islands were either totally unmethylated (37.5 % of the clones) or fully methylated (62.5 % of the clones). To corroborate that promoter methylation is the mechanism by which *Gpat2* expression is repressed in other tissues, genomic DNA from liver was bisulfite-modified and the *Gpat2* CpG island was sequenced. As expected, this region was totally methylated (results not shown). Thus, hypomethylation occurs at a specific time that is consistent with the initiation of meiosis (11 dpp) and precedes the maximum mRNA content detected at 15 dpp. Taken together, our data demonstrate that hypomethylation of the CpG island present in the *Gpat2* proximal promoter increases gene expression. A similar correlation between methylation status of the proximal promoter and gene expression was also observed for another member of the piRNA pathway, the mouse *Miwi* gene [25], whose temporospatial expression from midpachytene spermatocytes to round spermatids was associated with hypomethylation of the CpG island proximal promoter. Besides the spermatogenic cells, PIWI genes are overexpressed in some cancer types and this ectopic expression correlates with poorer clinical outcomes, suggesting that PIWI genes play a functional role in cancer biology [26]. Epigenetic mechanisms ensure the transient expression of the piRNA pathway genes at specific stages of spermatogenesis and their aberrant expression in somatic cancer cells [27]. Whether the expression of piRNAs and PIWI proteins in cancer is a consequence or a cause of malignancy remains unclear. However, it has been confirmed that the expression of piRNA pathway genes is essential for the progression of spermatogenesis, i.e. the disruption of *Miwi2* and *Mili* genes cause a meiotic-progression defect, loss of germ cells and sterility [28,29]. In our previous work, we confirmed not only the presence of human *GPAT2* in the cancer-derived cell line MDA-MB-231, but also its epigenetic regulation and relevance for the development of the tumour characteristics, since the GPAT2 knockdown dramatically decreased cellular proliferation, migration and *in vivo* tumorigenicity. In addition, on the basis of *in silico* information, high *GPAT2* expression occurs in human breast cancer, melanoma, lung cancer and prostate cancer [13].

Gpat2 gene transcription is up-regulated *in vitro* by retinoic acid

The varying expression of GPAT2 protein in mouse testis motivated us to search for hormone-responsive elements in its promoter region, particularly for those related to male sexual development and function. The promoter region used for analysis was the one selected for the −1324P construct, and the online program Alibaba 2.1 [30] was used to predict transcription factor-binding sites. This program uses the TRANSFAC public database, which contains an extensive compilation of published binding site data for eukaryotic transcription factors, their experimentally proven binding sites and regulated genes. For this region the program predicted seven glucocorticoid-response elements, nine retinoid-response elements [both retinoid X receptor (RXR) and RA receptor (RAR)], three oestrogen-response elements and two progesterone-response elements. We transfected the −1324P construct into cell lines that express the receptor for the hormone that was being evaluated. We tested *Gpat2* promoter activity with oestradiol, corticosterone and ATRA/9cisRA in MCF7, CHO-K1 or TM4 cell lines, respectively. No response was observed with oestradiol or corticosterone at the tested concentrations (results not shown). However, positive regulation was observed with two active vitamin A metabolites, 9cisRA and ATRA (Figures 5A and 5B). We observed that 8 μM 9cisRA and 10 μM ATRA duplicated −1324P activity (Figures 5A and 5B), but no synergistic effect was observed when both retinoids were present (results not shown). All the *Gpat2* active promoter constructs were up-regulated by both isomers of RA. Because both basal activity and the RA response decreased downstream of the −156P construct and because RA–retinoid receptor complexes usually interact with promoters near the transcription initiating site, it is possible that the predicted binding site for RA at +89 in the first intron might

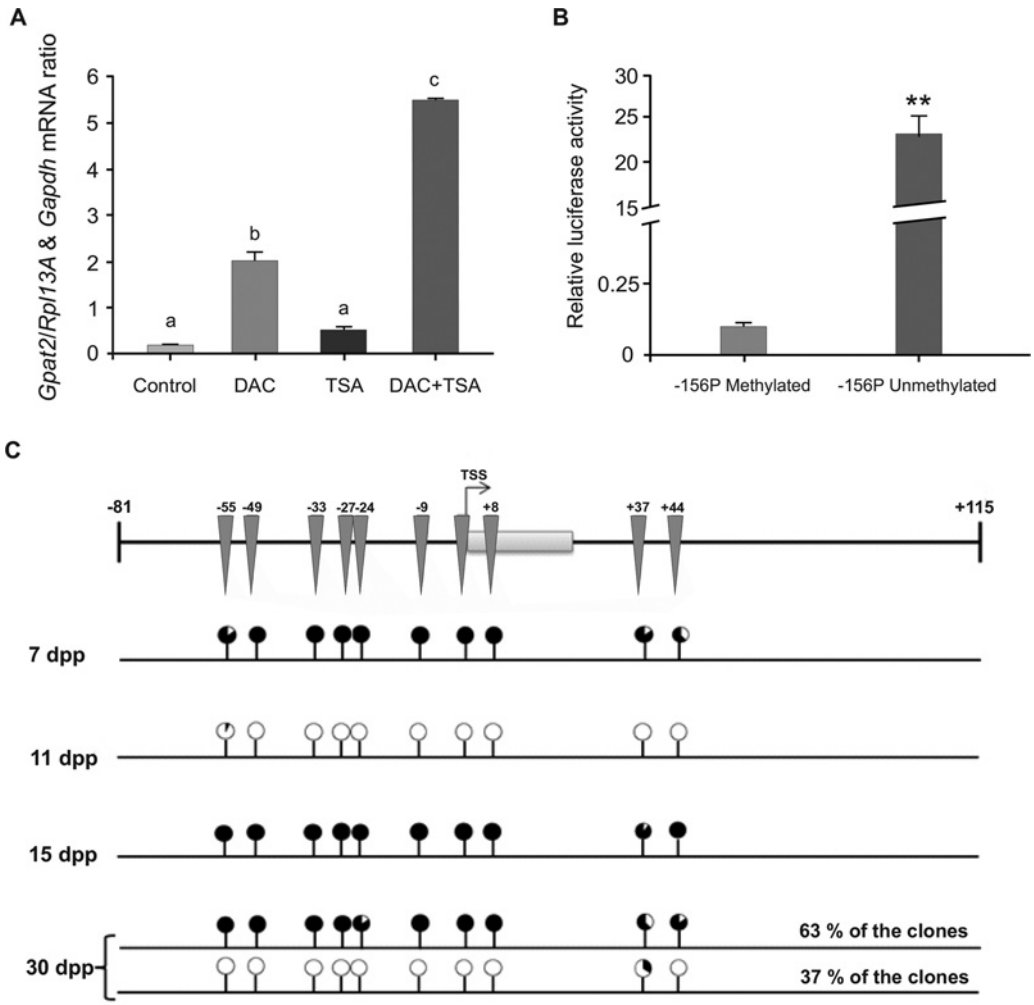

Figure 4 Epigenetic mechanisms involved in *Gpat2* transcription regulation

(**A**) The effect of the DNA methyltransferase inhibitor DAC and the histone deacetylase inhibitor TSA on *Gpat2* transcription on the murine cell line RAW 264.7 was assessed by qPCR and *Gpat2* mRNA relative expression level for each sample was normalized to its *Gapdh* and *Rpl13A* mRNA expression level. Bars with different letters indicate statistical difference ($P < 0.01$, one-way ANOVA and Tukey's test). (**B**) *In vitro* methylation of the *Gpat2* minimal promoter construct (− 156P) was performed and both methylated and unmethylated constructs were transfected into CHO-K1 cells. Promoter activity was measured as luciferase activity relative to the internal control *Renilla* luciferase (** $P < 0.01$, Student's *t* test). (**C**) Total DNA from 7 dpp testes or from isolated germ cells from 11, 15 and 30 dpp mouse testes was purified and bisulfite-modified, and the methylation status of the CpG island located on the proximal promoter region was analysed after PCR amplification and sequencing. The top bar shows a schematic representation of the location of CG pairs along the fragment that was amplified: inverted triangles represent the CG pairs and the grey box represents the first exon. Average methylation status of each position among all the sequenced clones is represented by circles: a black filled circle indicates that all cytosines were methylated at that position among all the clones (100 % methylated) and an empty circle indicates that all the cytosines were unmethylated at that position among all the clones (0 % methylated). Partially black circles indicate intermediate percentages of clones with a methylated cytosine at that position. The average methylation for each position is shown for 7, 11 and 15 dpp, considering all of the clones sequenced in each case (five to ten clones). However, at 30 dpp 37 % of the clones were almost fully unmethylated (10 % or less methylated cytosines) and 63 % were fully methylated (70 % or more methylated cytosines). Thus, at this age, the average methylation of each position is shown separately for the unmethylated clones (37 % of the clones) or the methylated ones (63 % of the clones) to emphasize the coexistence of two populations of germ cells in terms of *Gpat2* promoter methylation status at 30 dpp.

be involved in the *Gpat2* promoter retinoid response (Figures 5C and 5D).

Taking into account that RA synthesized endogenously by premeiotic spermatocytes autonomously induces meiotic initiation by controlling the RAR-dependent expression of *Stra8* [31] and that *Gpat2* expression correlates with the onset of prophase I of meiosis [at 13.5 dpc in ovaries (GEO profile GDS2223/1456208_at/Gpat2) and at 15 dpp in testes (Figure 1)] it could be speculated that RA may up-regulate *Gpat2* transcription *in vivo*. Increasing evidence demonstrates that ATRA influences the epigenetic environment regulating both DNA demethylation and histone acethylation/deacethylation [32–34]. Thus, the up-regulation of *Gpat2* expression by RA might be a consequence of promoter demethylation, histone deacetylation and/or canonical *trans*-activation. Further experiments are required to validate this hypothesis.

Gpat2 expression is not induced when 3T3-L1 fibroblasts are differentiated to adipocytes

Although *Gpat2* was initially cloned by its sequence homology to *Gpat1*, an enzyme that promotes triacylglycerol biosynthesis from endogenous and exogenous acyl-CoAs, primarily in liver [6], the role of GPAT2 in lipid metabolism remains controversial. We previously reported that LPA, the product of the GPAT-catalysed reaction, could not be detected when GPAT2 was overexpressed [14]. Overexpression of murine *Gpat2* in CHO-K1 cells shows no increase in GPAT activity when glycerol

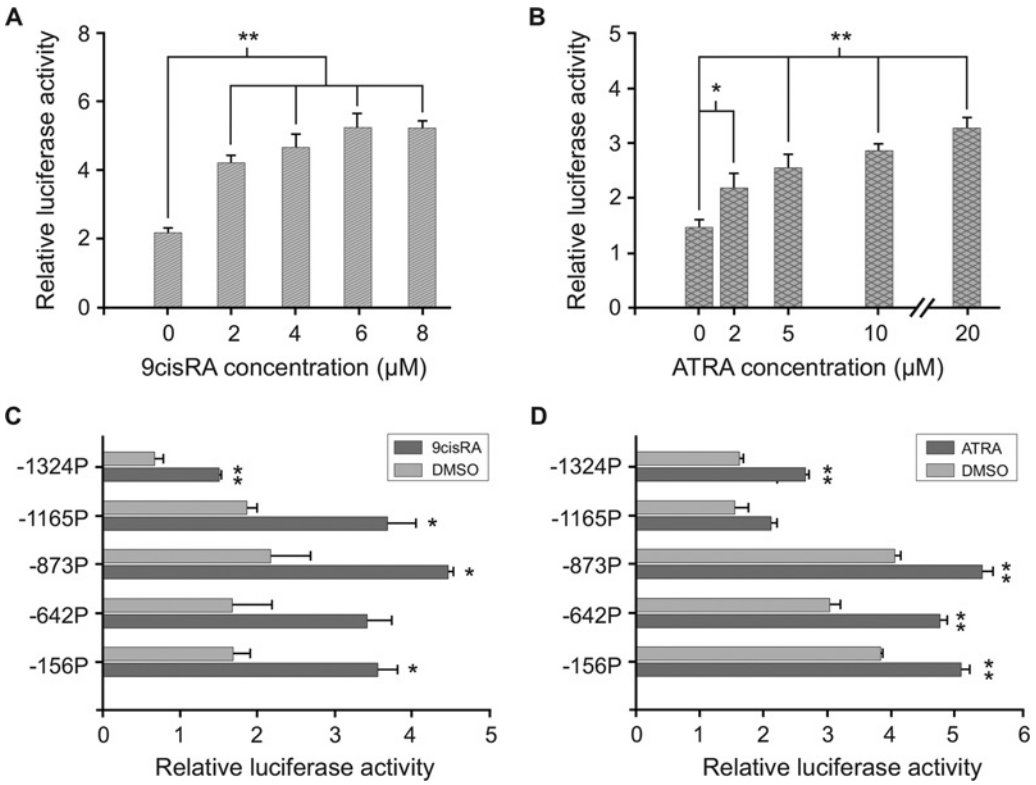

Figure 5 Retinoic acid up-regulates *Gpat2* promoter activity

The −1324P construct was transfected into TM4 cells and the effect of retinoids on *Gpat2* promoter activity was evaluated with 2, 4, 6 and 8 μM 9cisRA (**A**) and 2, 5, 10 and 20 μM ATRA (**B**). Both isomers significantly increased promoter activity (one-way ANOVA and Tukey's test), and 8 μM 9cisRA and 10 μM ATRA doubled it. (**C** and **D**) The effect of 9cisRA and ATRA on *Gpat2* active promoter constructs was tested: all were significantly up-regulated by both isomers of RA (Student's *t* test). Results represent means ± S.D. of the replicates from two independent experiments. ** $P < 0.01$, * $P < 0.05$. Luciferase activity is expressed relative to that of *Renilla* internal control.

3-phosphate and palmitoyl-CoA, oleoyl-CoA or linoleoyl-CoA are used as substrates; in contrast, a 2-fold increase in a chloroform-soluble product is observed when arachidonoyl-CoA is used as a substrate, although this increase is due to phosphatidic acid with no accumulation of LPA [14]. Moreover, *Gpat2* overexpression increases acylglycerol-3-phosphate acyltransferase activity when both oleoyl-CoA and arachidonoyl-CoA are used as substrates [14]. These results strongly suggest that GPAT2 may have an alternative acyltransferase activity. Additionally, GPAT2 expression is low in liver and adipose tissue, and fasting and refeeding do not alter the expression of murine *Gpat2* [10]. In order to determine whether GPAT2 might play a role in lipogenesis, its expression was assessed in differentiating 3T3-L1 mouse fibroblasts. No *Gpat2* mRNA induction was detected after cells differentiated into adipocytes (Figure 6), whereas, as expected, cells contained numerous large lipid droplets and a high content of TAG (results not shown). This result is consistent with the fact that the *Gpat2* promoter lacks binding sites for factors that regulate lipogenesis, such as the ones belonging to sterol-regulatory-element-binding protein 1 (SREBP1), cholesterol-regulatory-element-binding protein (ChREBP) or the peroxisome-proliferator-activated receptor (PPAR) family and suggests that the primary function of GPAT2 may be unrelated to the synthesis of triacylglycerol.

In conclusion, the expression of GPAT2 during spermatogenesis is consistent with the requirement for piRNA action and its transient expression is determined primarily by epigenetic modifications and possibly by RA, a key regulator of meiosis entry.

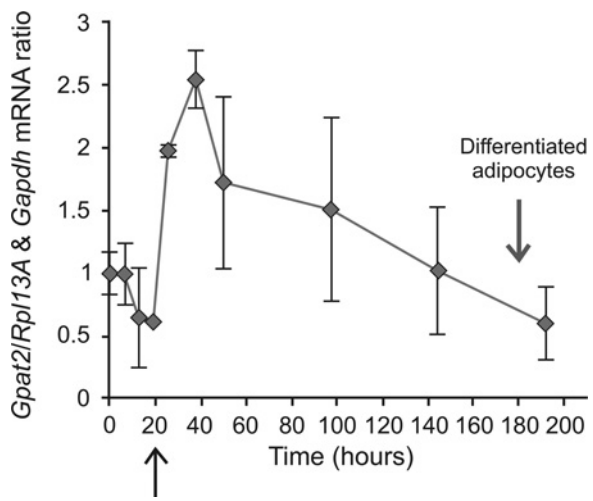

Figure 6 *Gpat2* expression decreases during 3T3-L1 differentiation into adipocytes

Gpat2 mRNA content was evaluated by qPCR during 3T3-L1 mouse fibroblasts differentiation into adipocytes and the *Gpat2* mRNA relative expression level for each sample was normalized to its *Gapdh* and *Rpl13A* mRNA expression level. The black arrow indicates the day when the differentiation cocktail was added. *Gpat2* mRNA content decreased after cell differentiation.

AUTHOR CONTRIBUTION

Magali Pellon-Maison, Maria Gonzalez-Baro, Mauro Montanaro, Maria Garcia-Fabiani conceived and designed the experiments. Maria Garcia-Fabiani, Mauro Montanaro,

Ezequiel Lacunza, Magali Pellon-Maison, Elizabeth Cattaneo performed the experiments. Maria Garcia-Fabiani, Maria Gonzalez-Baro, Magali Pellon-Maison, Mauro Montanaro, Ezequiel Lacunza analysed the data. Maria Gonzalez-Baro, Rosalind Coleman, Magali Pellon-Maison contributed reagents/materials/analysis tools. Magali Pellon-Maison, Maria Garcia-Fabiani, Maria Gonzalez-Baro, Rosalind Coleman, Mauro Montanaro wrote the paper.

ACKNOWLEDGEMENTS

We thank Mario Raul Ramos for the illustrations, Marianela Santana for her technical assistance and Dr Megumi Aita (UNC Molecular Neuroscience Core Facility) for her help with the *in situ* hybridization experiments.

FUNDING

This work was supported by the National Institutes of Health (NIH) [grant numbers 1R03TW008698 (to M.R.G.-B.) and R01DK56598 (to R.A.C.)]; the Agencia Nacional de Promoción Científica y Tecnológica (ANPCyT) [grant number PICT 2246 (to M.R.G.-B.)]; the Consejo Nacional de Investigaciones Científicas y Técnicas (CONICET) [grant number PIP0310 (to M.R.G.-B.)]; the UNLP [grant number M168 (to M.R.G.-B.)]; and the Universidad Nacional de La Plata (UNLP) [grant number PPIDM004 (to M.P.-M.)]. M.A.M., E.L., M.P.-M. and M.R.G.-B. are members of the Carrera del Investigador Científico y Tecnológico and MBGF is a fellow of CONICET, Argentina. The funders had no role in study design, data collection and analysis, decision to publish or preparation of the manuscript.

REFERENCES

1 Griswold, M.D., Hogarth, C.A., Bowles, J. and Koopman, P. (2012) Initiating meiosis: the case for retinoic acid. Biol. Reprod. **86**, 35 CrossRef PubMed
2 Hogarth, C.A. and Griswold, M.D. (2010) The key role of vitamin A in spermatogenesis. J. Clin. Invest. **120**, 956–962 CrossRef PubMed
3 Rajender, S., Avery, K. and Agarwal, A. (2011) Epigenetics, spermatogenesis and male infertility. Mutat. Res. **727**, 62–71 CrossRef PubMed
4 Aravin, A.A., Sachidanandam, R., Girard, A., Fejes-Toth, K. and Hannon, G.J. (2007) Developmentally regulated piRNA clusters implicate MILI in transposon control. Science **316**, 744–747 CrossRef PubMed
5 Shiromoto, Y., Kuramochi-Miyagawa, S., Daiba, A., Chuma, S., Katanaya, A., Katsumata, A., Nishimura, K., Ohtaka, M., Nakanishi, M., Nakamura, T. et al. (2013) GPAT2, a mitochondrial outer membrane protein, in piRNA biogenesis in germline stem cells. RNA **19**, 803–810 CrossRef PubMed
6 Wendel, A.A., Lewin, T.M. and Coleman, R.A. (2009) Glycerol-3-phosphate acyltransferases: rate limiting enzymes of triacylglycerol biosynthesis. Biochim. Biophys. Acta **1791**, 501–506 CrossRef PubMed
7 Jerkins, A.A., Liu, W.R., Lee, S. and Sul, H.S. (1995) Characterization of the murine mitochondrial glycerol-3-phosphate acyltransferase promoter. J. Biol. Chem. **270**, 1416–1421 CrossRef PubMed
8 Cao, J., Li, J.L., Li, D., Tobin, J.F. and Gimeno, R.E. (2006) Molecular identification of microsomal acyl-CoA:glycerol-3-phosphate acyltransferase, a key enzyme in *de novo* triacylglycerol synthesis. Proc. Natl. Acad. Sci. U.S.A. **103**, 19695–19700 CrossRef PubMed
9 Shan, D., Li, J.L., Wu, L., Li, D., Hurov, J., Tobin, J.F., Gimeno, R.E. and Cao, J. (2010) GPAT3 and GPAT4 are regulated by insulin-stimulated phosphorylation and play distinct roles in adipogenesis. J. Lipid Res. **51**, 1971–1981 CrossRef PubMed
10 Wang, S., Lee, D.P., Gong, N., Schwerbrock, N.M., Mashek, D.G., Gonzalez-Baro, M.R., Stapleton, C., Li, L.O., Lewin, T.M. and Coleman, R.A. (2007) Cloning and functional characterization of a novel mitochondrial *N*-ethylmaleimide-sensitive glycerol-3-phosphate acyltransferase (GPAT2). Arch. Biochem. Biophys. **465**, 347–358 CrossRef PubMed
11 Hofmann, O., Caballero, O.L., Stevenson, B.J., Chen, Y.T., Cohen, T., Chua, R., Maher, C.A., Panji, S., Schaefer, U., Kruger, A. et al. (2008) Genome-wide analysis of cancer/testis gene expression. Proc. Natl. Acad. Sci. U.S.A. **105**, 20422–20427 CrossRef PubMed
12 Whitehurst, A.W. (2014) Cause and consequence of cancer/testis antigen activation in cancer. Annu. Rev. Pharmacol. Toxicol. **54**, 251–272 CrossRef PubMed
13 Pellon-Maison, M., Montanaro, M.A., Lacunza, E., Garcia-Fabiani, M.B., Soler-Gerino, M.C., Cattaneo, E.R., Quiroga, I.Y., Abba, M.C., Coleman, R.A. and Gonzalez-Baro, M.R. (2014) Glycerol-3-phosphte acyltransferase 2 behaves as a cancer testis gene and promotes growth and tumorigenicity in the breast cancer MDA-MB-231 cell line. PLoS One **9**, e100896 CrossRef PubMed
14 Cattaneo, E.R., Pellon-Maison, M., Rabassa, M.E., Lacunza, E., Coleman, R.A. and Gonzalez-Baro, M.R. (2012) Glycerol-3-phosphate acyltransferase-2 is expressed in spermatic germ cells and incorporates arachidonic acid into triacylglycerols. PLoS One **7**, e42986 CrossRef PubMed
15 Coleman, R.A. and Bell, R.M. (1980) Selective changes in enzymes of the sn-glycerol 3-phosphate and dihydroxyacetone-phosphate pathways of triacylglycerol biosynthesis during differentiation of 3T3-L1 preadipocytes. J. Biol. Chem. **255**, 7681–7687 PubMed
16 Kobayashi, T., Suzuki, M., Morikawa, M., Kino, K., Tanuma, S. and Miyazawa, H. (2015) Transcriptional regulation of Tal2 gene by all-trans retinoic acid (atRA) in P19 cells. Biol. Pharm. Bull. **38**, 248–256 CrossRef PubMed
17 Boucheron, C. and Baxendale, V. (2012) Isolation and purification of murine male germ cells. Methods Mol. Biol. **825**, 59–66 CrossRef PubMed
18 Margolin, G., Khil, P.P., Kim, J., Bellani, M.A. and Camerini-Otero, R.D. (2014) Integrated transcriptome analysis of mouse spermatogenesis. BMC Genomics **15**, 39 CrossRef PubMed
19 Laiho, A., Kotaja, N., Gyenesei, A. and Sironen, A. (2013) Transcriptome profiling of the murine testis during the first wave of spermatogenesis. PLoS One **8**, e61558 CrossRef PubMed
20 Soumillon, M., Necsulea, A., Weier, M., Brawand, D., Zhang, X., Gu, H., Barthes, P., Kokkinaki, M., Nef, S., Gnirke, A. et al. (2013) Cellular source and mechanisms of high transcriptome complexity in the mammalian testis. Cell Rep. **3**, 2179–2190 CrossRef PubMed
21 Ku, H.Y. and Lin, H. (2014) PIWI proteins and their interactors in piRNA biogenesis, germline development and gene expression. Natl. Sci. Rev. **1**, 205–218 CrossRef PubMed
22 Beyret, E., Liu, N. and Lin, H. (2012) piRNA biogenesis during adult spermatogenesis in mice is independent of the ping-pong mechanism. Cell Res. **22**, 1429–1439 CrossRef PubMed
23 Gaunt, S.J. and Paul, Y.L. (2014) Synergistic action in P19 pluripotential cells of retinoic acid and Wnt3a on Cdx1 enhancer elements. Int. J. Dev. Biol. **58**, 307–314 CrossRef PubMed
24 Deaton, A.M. and Bird, A. (2011) CpG islands and the regulation of transcription. Genes Dev. **25**, 1010–1022
25 Hou, Y., Yuan, J., Zhou, X., Fu, X., Cheng, H. and Zhou, R. (2012) DNA demethylation and USF regulate the meiosis-specific expression of the mouse Miwi. PLoS Genet. **8**, e1002716 CrossRef PubMed
26 Moyano, M. and Stefani, G. (2015) piRNA involvement in genome stability and human cancer. J. Hematol. Oncol. **8**, 38–0133 CrossRef PubMed
27 Friemel, C., Ammerpohl, O., Gutwein, J., Schmutzler, A.G., Caliebe, A., Kautza, M., von Otte, S., Siebert, R. and Bens, S. (2014) Array-based DNA methylation profiling in male infertility reveals allele-specific DNA methylation in PIWIL1 and PIWIL2. Fertil. Steril. **101**, 1097–1103 CrossRef PubMed
28 Carmell, M.A., Girard, A., van de Kant, H.J., Bourc'his, D., Bestor, T.H., de Rooij, D.G. and Hannon, G.J. (2007) MIWI2 is essential for spermatogenesis and repression of transposons in the mouse male germline. Dev. Cell **12**, 503–514 CrossRef PubMed
29 Kuramochi-Miyagawa, S., Kimura, T., Ijiri, T.W., Isobe, T., Asada, N., Fujita, Y., Ikawa, M., Iwai, N., Okabe, M., Deng, W. et al. (2004) Mili, a mammalian member of PIWI family gene, is essential for spermatogenesis. Development **131**, 839–849 CrossRef PubMed
30 Wingender, E., Chen, X., Hehl, R., Karas, H., Liebich, I., Matys, V., Meinhardt, T., Pruss, M., Reuter, I. and Schacherer, F. (2000) TRANSFAC: an integrated system for gene expression regulation. Nucleic Acids Res. **28**, 316–319 CrossRef PubMed
31 Raverdeau, M., Gely-Pernot, A., Feret, B., Dennefeld, C., Benoit, G., Davidson, I., Chambon, P., Mark, M. and Ghyselinck, N.B. (2012) Retinoic acid induces Sertoli cell paracrine signals for spermatogonia differentiation but cell autonomously drives spermatocyte meiosis. Proc. Natl. Acad. Sci. U.S.A. **109**, 16582–16587 CrossRef PubMed
32 Rowling, M.J., McMullen, M.H. and Schalinske, K.L. (2002) Vitamin A and its derivatives induce hepatic glycine *N*-methyltransferase and hypomethylation of DNA in rats. J. Nutr. **132**, 365–369 PubMed
33 Lim, J.S., Park, S.H. and Jang, K.L. (2011) All-trans retinoic acid induces cellular senescence by up-regulating levels of p16 and p21 via promoter hypomethylation. Biochem. Biophys. Res. Commun. **412**, 500–505 CrossRef PubMed
34 Heo, S.H., Kwak, J. and Jang, K.L. (2015) All-trans retinoic acid induces p53-depenent apoptosis in human hepatocytes by activating p14 expression via promoter hypomethylation. Cancer Lett. **362**, 139–148 CrossRef PubMed

Received 26 June 2015/11 August 2015; accepted 12 August 2015
Accepted Manuscript online 12 August 2015, doi:10.1042/BJ20150730